Proceedings of the 2025 SICE Festival with Annual Conference
September 9-12, 2025, Chiang Mai, Thailand

Development of a Snake-like Robot Designed for Coiling and Compression Movements for DVT Prevention

Mei Kubota[1†] and Tomoyuki Yamaguchi[2]

[1]University of Tsukuba, Ibaraki, Japan
(Tel: +81-029-853-5459; E-mail: kubota@ice.iit.tsukuba.ac.jp)
[2]University of Tsukuba, Ibaraki, Japan
(E-mail: yamaguchi@iit.tsukuba.ac.jp)

Abstract: Prolonged periods of immobility can lead to the formation of blood clots, a condition known as economy class syndrome or deep vein thrombosis (DVT). There is a high risk of DVT in confined spaces, including long flights, buses and evacuation centers. Prior studies have introduced electrostimulation devices that are clinically proven to promote blood flow. However, these devices cannot be reused and must be attached to the appropriate position by the user. Other types of massage devices, including stationary and wearable massagers, have been developed; however, they require installation space, wearing motion, and soundproofing measures in a small space, and have portability issues. To address these challenges, this study presents a small, snake-shaped robot that performs a compression motion by coiling itself around a target through shape control. In this paper, we propose a modeling method for controlling the robot's shape to enable coiling around the target and a method for compression motion control aiming at a target pressure of 30-60mmHg—similar to the intermittent pneumatic compression (IPC) device used in hospitals. Through the experiment, we confirmed that the results for the coiling motion revealed that the robot coiled around the target by curling its body with increasing tension. As for the compression motion, the compression also increased with increasing tension, eventually reaching an average of 30mmHg.

Keywords: Snake-like Robot, Deep Vein Thrombosis (DVT), Physical Care, Compression Therapy

1. INTRODUCTION

In recent years, the occurrence of frequent natural disasters has forced many people to seek refuge in evacuation shelters [1]. This has led to serious health risks associated with prolonged duration in overcrowded shelters [2]. Among these, the economy class syndrome or deep vein thrombosis (DVT)—caused by prolonged exposure to the same posture—has become a new health threat. If a blood clot dislodges and reaches the lungs, it can lead to pulmonary embolism, which is a serious condition [3]. Therefore, hospitals employ elastic stockings and intermittent pneumatic compression (IPC) devices, which have proven effective in preventing DVT, since it is necessary to maintain the same posture for long periods during surgery [4]. Elastic stockings promote blood circulation by applying pressure in stages starting at the ankle, and physicians may recommend that patients wear these stockings continuously over 24 hours [5][6]. IPC is applied to patients at high risk of blood clot formation and promotes blood circulation by applying air pressure compression.

However, DVT is not limited to hospital settings, and can be encountered in various situations in daily life, such as in evacuation centers, on long-distance flights, and in night buses and cars. While the methods used in hospitals have been shown to be effective, proper application requires specialized knowledge. Incorrect use reduces effectiveness and carries the risk of complications, such as skin damage and blood circulation problems. Therefore, there exists a strong need for easier preventive measures in situations where proper use of medical devices is difficult.

Therefore, the Ministry of Health, Labour and Welfare (MHLW) generally recommends physical care, such as light exercises and calf massage, as illustrated in Fig. 1, as preventive measures against DVT [3]. These methods are useful because they can be performed independently and do not require specialized knowledge or tools to promote blood flow. However, it is difficult to encourage continuous exercise in situations such as living in a shelter or traveling for long hours.

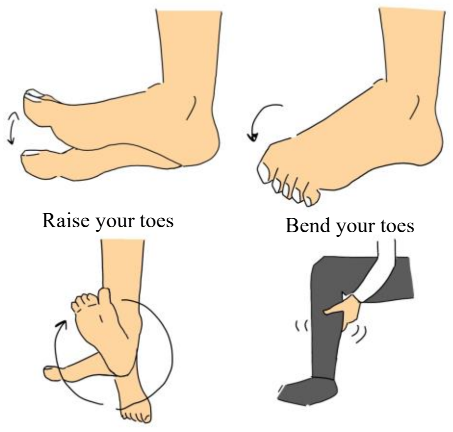

Fig. 1 Examples of physical care.

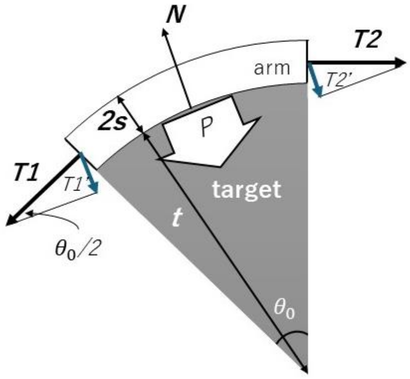

Fig. 2 Compression action control minute range.

There are three approaches to address this problem: the stationary approach in which the feet are placed in a commercially available massager to promote blood flow; the wearable device approach in which the device coils around the entire foot [7]; and the massage gun approach that massages and relaxes the entire body. However, they are not suitable for use in confined spaces such as shelters, cars, and night buses because they require installation space, wearing motion, and soundproofing measures; additionally, they are difficult to carry around.

Another study proposed the *geko* device, which has been clinically proven to activate leg muscles and increase blood flow through electrical stimulation [8]. The *geko* device is a small, wearable medical device with a lightweight design that can be used in confined spaces and allows a high degree of physical freedom during use, making it suitable for continuous use in shelters and during long travels.. However, they cannot be reused in evacuation centers where many people gather because they are disposable and must be attached to the appropriate position by the user. They are difficult to use on subjects who are unaware of their DVT risk. Thus, this method does not satisfy all three requirements: versatility for use by various people, miniaturization of the device, and active prevention of DVT by the device.

Therefore, this study focuses on "give yourself a calf massage," one of the recommendations by the Ministry of Health, Labour and Welfare, as illustrated in Fig. 1, and proposes a small snake-shaped robot that actively coils around the target to autonomously perform a massage by controlling the robot's shape. The robot comprises a small mechanism consisting of a set of motors, wires, and multiple joints. Because the robot is multi-jointed, it can flexibly respond to different sizes of the target to be coiled around. Coiling and proper compression are essential for a snake-like robot to massage the calf. In particular, assuming physical care to the calf area, the two necessary motion controls are "shape control" of the body that coils around the target and "compression motion control" that compresses the target. In shape control, the body must be appropriately rounded according to calf thickness. In the compression motion, compression pressure in the range of 30-60 mmHg used in common IPC devices is required [9].

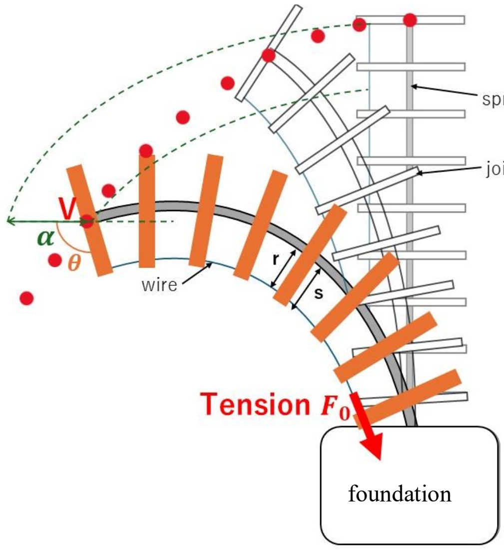

Fig. 3 Overall diagram of shape change.

In this study, shape control and pressure motion control for a snake-shaped robot were modeled, and the robot was developed. The accuracy of the shape control of the developed robot and its ability to achieve the target compression pressure were tested experimentally, and an evaluation was conducted to demonstrate the effectiveness of the proposed robot.

2. CONTROL METHOD FOR THE SNAKE-LIKE ROBOT

While various methods have been proposed for snake-like robots, this study refers to a wire model that enables shape control of an articulated robot by manipulating wires [10]. In this study, we first designed a snake-shaped robot that can realize physical care by "leaning on the calf" through simple bending operations using a single wire and then performing shape control.

To realize the "calf massage" action, it is necessary to apply appropriate pressure to the calf while it is coiled around it. Therefore, the snakelike robot was designed separately for shape control to coil around the leg, similar to a robot frame, and for compression motion control to massage the leg. The symbols used are as follows:

i=1,2,3…,9: Order in which joints are counted from the base
α: Amount of wire manipulation when operating with the tip joint restrained
V: Position of the tip joint
θ: Tilt angle of the tip joint
r: Distance from the center axis of the frame to the wire
h: Distance between joints
t: Radius of the object to be coiled around
F_0: Magnitude of the wire tension in shape control
M_0: Bending moment generated by the wire operation
EI: Bending rigidity
D: Number of joints
s: Distance from the center of frame to the joint end

T1 (*T2*): Tension vector applied to one end of the frame
T1' (T2'): Minute force toward the center of *T1 (T2)*
F_1: Magnitude of the tension vector of the wire in the compression motion control
T: Combined force of *T1'* and *T2'*
P: Pressure applied by the frame to the object
N: Vertical drag force of the force applied when the frame coils around the object
n: Number of joints deformed
θ_0: Center angle in the small range shown in Fig. 2.

2.1 Shape Control

For shape control, it is necessary to clarify the relationship between the amount of wire manipulation and the tip position. In a previous study [10], assuming no gravity and no frame elongation, the tip position was expressed as described in equation (1) (Fig. 3).

$$(x,z) = \left(\frac{Dh}{2r}\alpha\,, Dh - \frac{(D^2-1)h}{6Dr^2}\alpha^2\right), \theta = \frac{\alpha}{r} \quad (1)$$

Thus, the tip position depends on the extent of wire manipulation. Assuming that n is the number of joints that are deformed because of the effect of gravity out of the number of joints *D*, *n*=5 was used in the calculation instead of *D*. It is necessary to clarify the wire tension F_0 to control the amount of wire manipulation. According to a previous study [10], wire tension F_0 is as follows:

$$F_0 = \frac{EI}{Dhr^2}\alpha \quad (2)$$

D, h, and *r* were set according to the snake-like robot to be manufactured. *EI*, which is an unknown number, was obtained analytically through experiments. From the above, the relationship between the wire tension amount *α* and the wire tension F_0 is shown.

2.2 Compression motion control

Clarifying the relationship between the target compression pressure P and the magnitude of tension T is necessary to control the compression motion. We assume that no frictional force acts between the object and the frame. The forces acting on a small area of the coiled frame are illustrated in Fig. 2. All forces *T1, T2*, and *N* on the frame were balanced. The combined force *T* and vertical drag force *N* are expressed as follows:

$$T = T1' + T2' = 2F_1 sin\frac{\theta_0}{2} \quad (3)$$

$$N = Pt\theta_0 \times 2s \quad (4)$$

Taking the limit $\theta_0 \to 0$ from *T=N*, the tension magnitude F_1 is as follows:

$$2F_1\sin\frac{\theta_0}{2} = 2Pts\theta_0 \to F_1 = 2Pts \quad (5)$$

From equation (5), F_1 has a magnitude proportional to pressure *P*. Set *t* and *s* according to the snake-shaped robot to be manufactured. This shows the relationship between the pressure *P* applied by the frame and the tension F_1.

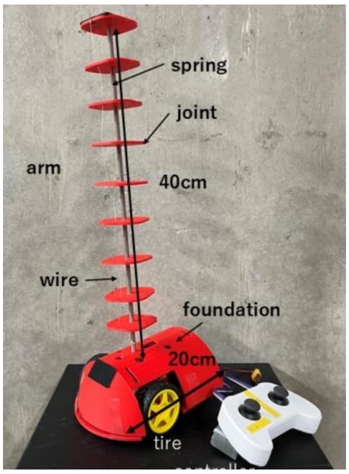

Fig. 4 Snake-like robot.

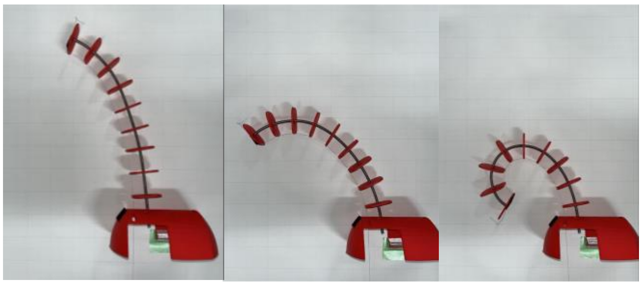
Fig. 5 Horizontal state.

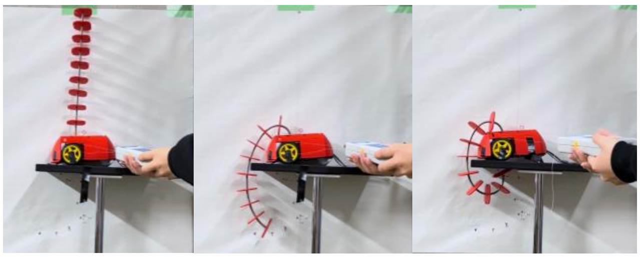
Fig. 6 Under gravity.

3. DEVELOPMENT OF THE SNAKE-LIKE ROBOT

3.1 Design of the snake-like robot

Because the compression pressure of common IPC devices is set at 30-60 mmHg [11], the target pressure was set at 40 mmHg with reference to the major IPCs. The fabricated snake-shaped robot is illustrated in Fig. 4. This robot has a wire-driven structure with joints and compression springs, and a gear motor is used to realize the coiling motion. Based on equation (2), an increase in the number of joints reduces the tension required for shape control; however, it also increases the complexity of the control and the weight. Therefore, the number of joints was determined to be nine, referring to a snake-like robot that can move in a pipe-like environment, as reported in a related study [11]. Considering the maximum circumference of the calf, which was the objective, a 40 cm spring was adopted as the central axis of the frame.

3.2 Analysis of bending stiffness EI

EI, the unknown in equation (2), was obtained analytically. A fabricated snake-shaped robot with D = 9, Dh = 40 cm, and r = 2.5 cm was used. The bending rigidity was obtained from the results of five trials in which the wire tension α was varied in 1 cm increments, and the corresponding tension F_0 was measured and averaged as follows, which is a fixed value.

$$EI = \frac{F_0 Dhr^2}{\alpha} = 65.11N * cm^2 \quad (6)$$

3.3 Motor Selection

The wire tension was determined by shape control and compression motion control, and the appropriate motor was determined based on the wire tension. The parameters used are: r = 2.5 cm, D = 9 pieces, Dh = 40 cm, t = 5.5 cm, EI = 65.11 $N \cdot cm^2$.

1) Tension in shape control

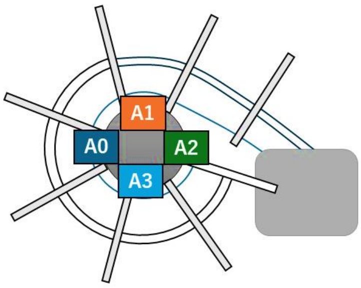

Fig. 7 Pressure sensor mounting location.

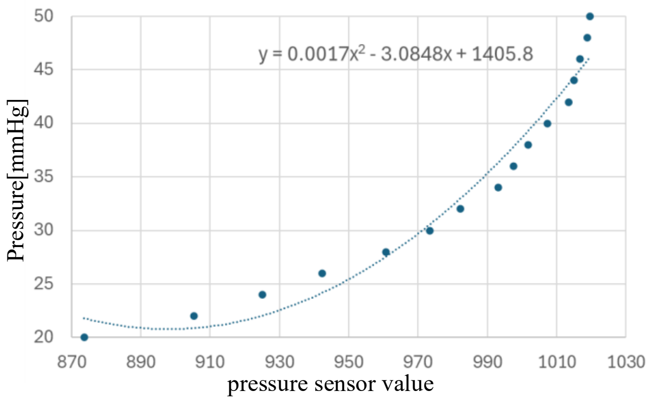

Fig. 8 Pressure sensor characteristics.

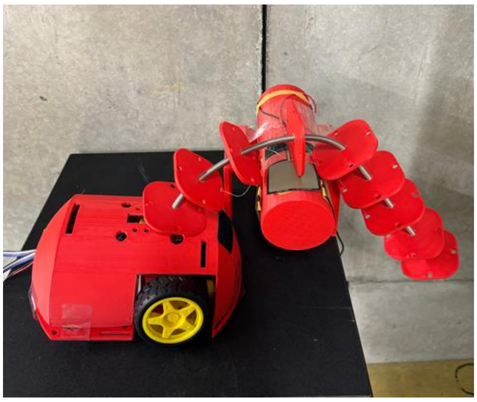

Fig. 9 Compression control.

The wire operation amount α increases with an increase in the tilt angle θ of the tip joint. From equation (3), the amount of wire manipulation α = 2.5θ. From equation (2), the tension in the shape control is F_0 = 0.75θ. The change in tension F_0 until the frame coils around the object ($\theta = 2\pi$) increases monotonically, and the tension takes the maximum value F_0 = 2.36N at θ = 2π.

2) Tension in compression motion control

The tension in the case of a coiling around the ankle model was determined. From equation (5), the wire tension F_1 = 0.0015P. If a target compression pressure of 40 mmHg is set, tension F_1 is 8.0 N.

Thus, the greatest tension is required at F_1=8.0N when the compression operation is completed. At this time, the required torque τ is 0.82 kgf·cm, based on the wheel radius of 0.01 m.

Consequently, a gearmotor with a stopping torque of 15 kgf·cm, a no-load speed of 20 rpm, and a rated voltage of 12 V was selected for the design.

4. EXPERIMENTS

To test the validity of the proposed control methods, experiments were conducted with the frame fixed in two states, horizontal (Fig. 5) and upright (Fig. 6).

4.1 Experimental Methods

(1) Shape control verification experiment

The relationship between the tension force and tip position was compared with the theoretical values to verify the validity of the relationship. The experiment was conducted as follows.

1) A force gauge was attached to the tip of the wire.

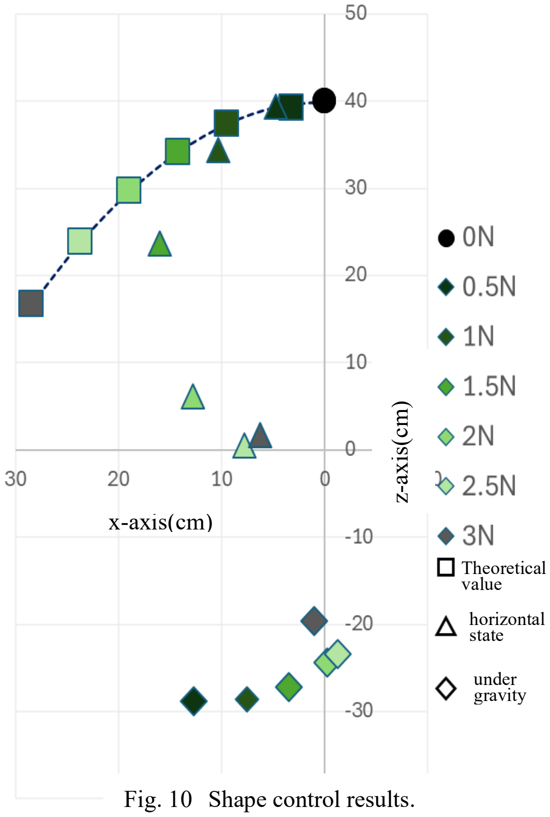

Fig. 10 Shape control results.

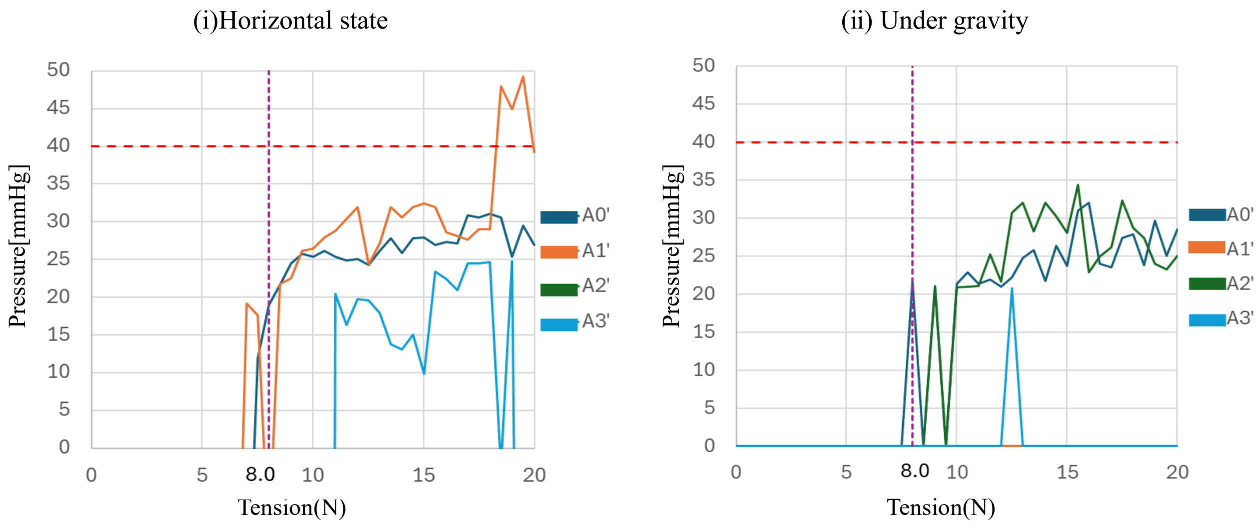

Fig. 11 Compression action control results.

2) A graph paper was placed on the back of the frame such that the tip position could be recorded using the root as the origin.

3) The force gauge was manually operated to apply tension to the wire.

4) The tension was varied in 0.5N increments, and the tip position was recorded on the graph paper by maintaining the state at that point by hand.

5) The measurement results were compared with theoretical values to verify and discuss their validity.

The target theoretical value was set to $r = 2.5$ cm, $n = 5$, $Dh = 40$ cm, $t = 5.5$ cm, and $EI = 65.11\ N \cdot cm^2$ using equation (1). The theoretical value of the tip position in relation to the tension is expressed by the following equation:

$$x = \frac{nh}{2r}\left(\frac{nhr^2}{EI}F_0\right) \approx 9.48F_0\ cm \quad (7)$$

$$z = Dh - \frac{(n^2-1)h}{6nr^2}\left(\frac{nhr^2}{EI}F_0\right)^2 \approx 40 - 2.59{F_0}^2\ cm \quad (8)$$

(2) Compression Motion Control Verification Experiment

The measured results were compared with theoretical values to validate the relationship between tension and pressure. A cylindrical ankle model with a diameter of 6 cm and a height of 20 cm was used for the experiment. Four pressure sensors were placed on the sides of the model at the positions illustrated in Fig. 7. Pressure sensor A2 was located at the tip of the frame, and A3, A0, and A1 were arranged sequentially toward the base of the frame. The pressure sensors used followed the sensor characteristics depicted in Fig. 8. In this study, the pressure value range was set to 20 to 50 mmHg. Within this range, the pressure sensor values were confined to fall between 873.6 and 1019.6. The pressure sensor values were converted to pressures [mmHg] using the approximate curve in Fig. 8 and were recorded as A0', A1', A2', and A3'. To ensure consistency beyond the measured range, this curve was created using a quadratic equation, and the maximum error between the measured values and the approximation was 3.78 mmHg at an applied pressure of 50 mmHg. The values outside the range of 873.6-1019.6 were regarded as error values and processed as 0. The experiment was conducted as follows.

1) A force gauge was attached to the end of a wire.

2) The ankle model was fixed and positioned such that the snake-like robot could coil around along its side.

3) The force gauge was manually operated to apply tension to the wire.

4) The tension was varied in 0.5N increments, and the value of each pressure sensor on the calf model at that point was recorded.

5) The measured results were compared with theoretical values to verify and discuss validity.

Confirmation that the target pressure of 40 mmHg was reached at 8.0 N of tension. The actual compression motion control experiment is shown in Fig. 9.

4.2 Results and Discussions

(1) Shape control verification experiment

The results are shown in Fig. 10. The results under gravity differ from the theoretical value; however, the frame droops once under the influence of gravity and deforms to a rounded shape at a tension of 2.36N required for the frame to form a full circle. In the horizontal state, a difference from the theoretical value was observed as the tension increased; however, the tip was rounded and a suitable coiled shape was confirmed.

Because the frame can be round and coil around in the actual measurement, it is necessary to revisit the control methods considering the change in spring bending rigidity. Future improvements include increasing the rigidity of the frame, improving measurement accuracy, and constructing a control methods that considers gravity. This enabled us to obtain results closer to the theoretical values; additionally, the number of wires should be increased to achieve uniform and stable compression using only the motor.

(2) Experimental verification of pressure motion control

Fig. 11 displays a graph of the actual measured values in terms of tension and pressure sensor values. From Fig. 7, the pressure sensors are positioned at A0' on the calf model, which is the farthest from the base, and are arranged clockwise as A1', A2', and A3'. To achieve stable compression, it is necessary to evenly increase the pressure of opposing sensors (such as A0' and A2'). The left side shows the results measured in the (i) horizontal condition, with the bottom part of the figure focusing on the data showing pressures of 0 mmHg or greater. The right side shows the results of (ii) under gravity, and similarly shows the overall graph at the top and data showing pressures above 0 mmHg at the bottom. The results showed that regardless of the effect of gravity, pressure sensors A0' and A1' showed stable and high output after 10N, and a compression equivalent to 30 mmHg was achieved. This corresponds to the pressure range within which IPC is effective in promoting blood flow. Pressure sensor A2' at the end of the frame showed unstable compression. A3', whose frame was sensitive to the direction of gravity, showed stable compression in the horizontal state; however, under gravity, unstable compression was observed, as in A2'.

Although a target pressure of 40 mmHg could not be reached at a theoretical tension of 8.0 N due to contact surface variation and spring elongation, it can be said that a single-wire drive is effective in promoting blood flow if an appropriate tension is applied correctly such as changing the spine materials. The snake-like robot proposed in this study only has a shape-changing mechanism; however, to achieve 40 mmHg, the introduction of an airbag, which is a pressurization mechanism, would be effective. Further, a tubular airbag could solve the problem of poor contact.

5. SUMMARY

Aiming to develop a physical care robot for DVT prevention, this study verified the shape and pressure motion control of a snake-shaped robot that coils around the calf and compresses it. Frame bending and pressure increase due to wire tension were confirmed; however, the results deviated from the theoretical values, which were influenced by gravity, aircraft weight and friction, changes in bending rigidity, and variations in contact surfaces. Future research will include the introduction of airbags, the establishment of a method to identify care recipients, and incorporation of various types of physical care.

ACKNOWLEDGEMENT

This work was partially supported by JSPS Grant-in-Aid for Scientific Research(B) Grant Number 23K26337.

REFERENCES

[1] White Paper on Land and Transportation 2020, https://www.mlit.go.jp/hakusyo/mlit/r01/hakusho/r02/html/n1222000.html

[2] Residential Environment Value Improvement Business Cooperative, "Problems faced by shelters," http://www.sarex.or.jp/chie/chiebukuro_3.pdf

[3] Ministry of Health, Labour and Welfare, "To prevent economy class syndrome," https://www.mhlw.go.jp/stf/seisakunitsuite/bunya/0000170807.html

[4] M. Ito, "Guidelines for Diagnosis, Treatment and Prevention of Pulmonary Thromboembolism and Deep Vein Thrombosis," pp. 52-67, 2020.

[5] Tokyo Vascular & Vein Clinic, "Elastic stockings Prevention of blood clots Swelling Lymphedema," https://www.tokyokekkan.com/efforts/stockings/.

[6] Meguro Surgery, "Elastic stockings for sleeping," https://meguro-geka.jp/joumyakuryu blog/compressionstocking-sleeping/

[7] ZEWELLDA, "3 levels of calf relaxing foot care," https://www.amazon.co.jp/dp/B0CGZPFRF4?tag=mybest_presses_ 21806_90-22

[8] H. Jawad, Duncan S. Bain,Helen dawson, Kate crawford, Atholl Johnston, Arthur Tucker, "The effectiveness of a novel neuromuscular electrostimulation method versus intermittent pneumatic compression in enhancing lower limb blood flow," *Journal of Vascular Surgery Venous and Lymphatic Disorders*, Vol. 2, No. 2, pp. 160-165, 2013.

[9] The Japanese Phlebological Society, "Guidelines for Compression Therapy in Venous Disease," 2024.

[10] Y. Hayashi, M. Yamamoto, "Shape Control of Hose-like Flexible Arm by Wire's Constrains," *Transactions of the Japan Society of Mechanical Engineers. C* ,Vol. 7, No. 4, pp. 153-160, 2007

[11] Hirose Shigeo, Yamada Hiroya, "Snake-Like Robots," *IEEE Robotics & Automation Magazine*, Vol. 16, No. 1, pp. 88-98, 2009.